

Anomalous tropical ocean circulation associated with La Niña Modoki

Toshiaki Shinoda,¹ Harley E. Hurlburt,¹ and E. Joseph Metzger¹

Received 18 May 2011; revised 12 September 2011; accepted 13 September 2011; published 2 December 2011.

[1] El Niño Modoki is a variant of El Niño characterized by warming around the dateline flanked by anomalous cooling in the east and west. However, the opposite phase (La Niña Modoki) has received little attention because the prominent cooling of sea surface temperature (SST) during major La Niña events is observed in the central Pacific, and thus, it is difficult to define the two different types of cold events from the SST anomaly pattern. Here we demonstrate that cold events in 2000 and 2008 can be clearly distinguished from traditional La Niña events using surface currents derived from satellite observations. During 2000 and 2008, anomalous zonal currents in the equatorial Pacific demonstrate divergence, with westward currents west of the dateline and eastward currents east of it. These currents are opposite to the circulation pattern during the 2004 El Niño Modoki event. An empirical orthogonal function (EOF) analysis of surface currents for the period 1993–2009 shows a circulation anomaly pattern similar to that in 2000, 2004, and 2008 in the second EOF. The first EOF is consistent with traditional El Niño/La Niña events and does not exhibit a current reversal along the equator. Our results also indicate that strong cyclonic (anticyclonic) circulation anomalies occur in the tropical western Pacific around 5°N–15°N during the 2004 (2000 and 2008) El Niño (La Niña) Modoki events and during the strong traditional El Niño (La Niña) events of 1997 (1998). These circulation anomalies are related to an SST gradient in the western and central Pacific.

Citation: Shinoda, T., H. E. Hurlburt, and E. J. Metzger (2011), Anomalous tropical ocean circulation associated with La Niña Modoki, *J. Geophys. Res.*, 116, C12001, doi:10.1029/2011JC007304.

1. Introduction

[2] El Niño [e.g., Rasmusson and Carpenter, 1982; Philander, 1983], which is characterized by unusually warm temperature in the eastern Pacific Ocean, impacts climatic conditions in many regions of the globe [e.g., Horel and Wallace, 1981; Ropelewski and Halpert, 1987; Alexander *et al.*, 2002]. In recent years, the patterns of sea surface temperature (SST) warming in the tropical Pacific associated with El Niño seem to be changing [Ashok *et al.*, 2007]. Since the 1970s, there have been some warm events in the Pacific Ocean where the maximum SST anomaly is located in the central Pacific and is flanked by anomalous cold SSTs at the western and eastern ends of the equatorial Pacific. Recent studies have classified the warm events with the alternative SST anomaly pattern as a new type of El Niño, named El Niño Modoki [Ashok *et al.*, 2007], a pattern which has different impacts on global climate through teleconnection [e.g., Ashok *et al.*, 2007; Trenberth and Stepaniak, 2001; Kumar *et al.*, 2006; Wang and Hendon, 2007; Weng *et al.*, 2009]. Other names, such as Dateline El Niño [Larkin and Harrison, 2005], Central Pacific El Niño [Kao and Yu, 2009], and Warm Pool El Niño [Kug *et al.*,

2009] have been used for this phenomenon with slightly different viewpoints. The recent increased occurrence of El Niño Modoki events could possibly be attributed to changes in the zonal slope of the equatorial thermocline caused by global warming since the late 1970s [Ashok *et al.*, 2007; Yeh *et al.*, 2009].

[3] The opposite [La Niña; Philander, 1985] phase of El Niño, which is characterized by cold SST anomalies in the equatorial Pacific, also affects tropical and extratropical climate variability, including shifts in tropical rainfall and wind patterns at middle and high latitudes [e.g., Hoerling *et al.*, 1997]. However, the changes in characteristics of La Niña have not been emphasized because the SST anomaly pattern during cold events in recent years is not distinctly different from the “canonical” La Niña events.

[4] The difference in SST anomaly pattern between El Niño–Southern Oscillation (ENSO) cold and warm events is documented in previous studies [e.g., Larkin and Harrison, 2002; McPhaden and Zhang, 2009]. This difference is clearly shown in composite SST anomalies from the last 29 years based on the frequently used ENSO index (Niño3.4 SST; Figure 1). Large warm anomalies comparable to those at the eastern edge of the Niño3.4 region (120°W) are found near the eastern boundary in the El Niño composite (Figure 1a), while strong cold anomalies in the western Pacific extend nearly to 160°E in the La Niña composite (Figure 1b). This remarkable difference in SST

¹Naval Research Laboratory, Stennis Space Center, Mississippi, USA.

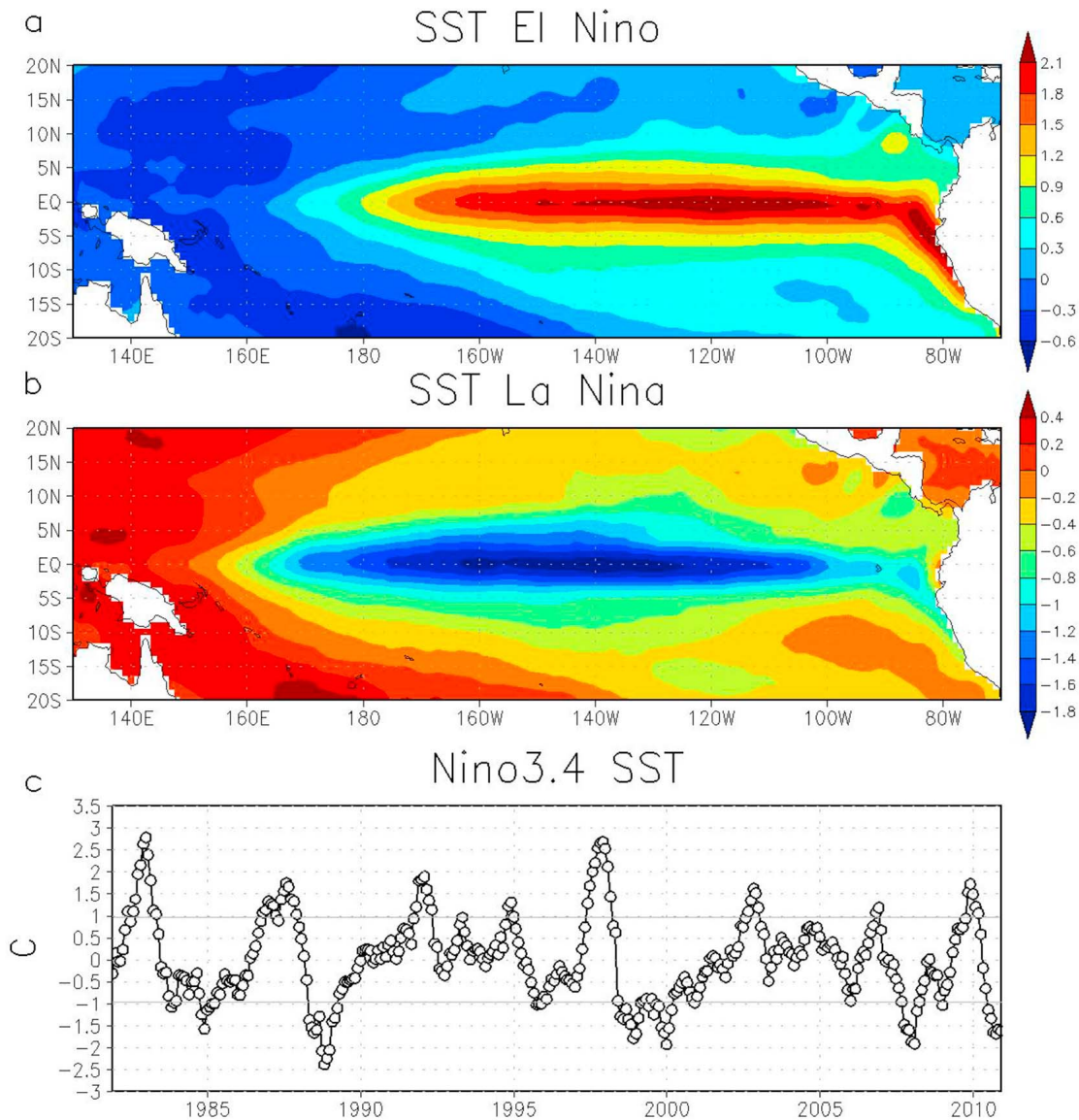


Figure 1. Composite SST anomalies for (a) El Niño and (b) La Niña. The periods of El Niño (La Niña) are defined as the months when the positive (negative) SST anomaly in the Niño3.4 area (170°W – 120°W , 5°N – 5°S) exceeds one standard deviation. (c) Time series of monthly Niño3.4 SST anomaly. The horizontal lines indicate one standard deviation.

anomaly pattern between cold and warm events is also clearly evident in individual major El Niño and La Niña events. For example, during one of the strongest La Niña events in 1988, the coldest SST anomaly was located around 130°W – 120°W and significant SST anomalies extended as far west as 160°E in the western Pacific (Figure 2a). This SST anomaly pattern is completely different from that during the two strongest El Niño events in 1982–1983 and 1997–1998, where the maximum SST anomaly is observed near the eastern boundary (Figures 2c and 2d). The large cold SST anomalies during another strong La Niña event in 1998–1999 were located around 140°W , and comparable SST anomalies were found in the central Pacific near the dateline (Figure 2b). While this anomaly pattern is some-

what different from that of the 1988–1989 La Niña event, it is not at all similar to the major El Niño events in 1997–1998 and 1982–1983. Because of this asymmetry in the SST anomaly pattern between the warm and cold events, it is difficult to clearly distinguish the two types of La Niña from the spatial pattern of SST. In fact, indices for both El Niño (Niño3.4 SST) and El Niño Modoki (ENSO Modoki index (EMI)) are much lower than average during these La Niña events in 1988 and 1998 [Ashok *et al.*, 2007]. Also, the SST anomalies near the dateline are very strong during these La Niña years, while they are nearly normal during the strong El Niño years in 1982 and 1997.

[5] In this study, we analyzed a variety of data from satellite observations to identify distinct spatial patterns of

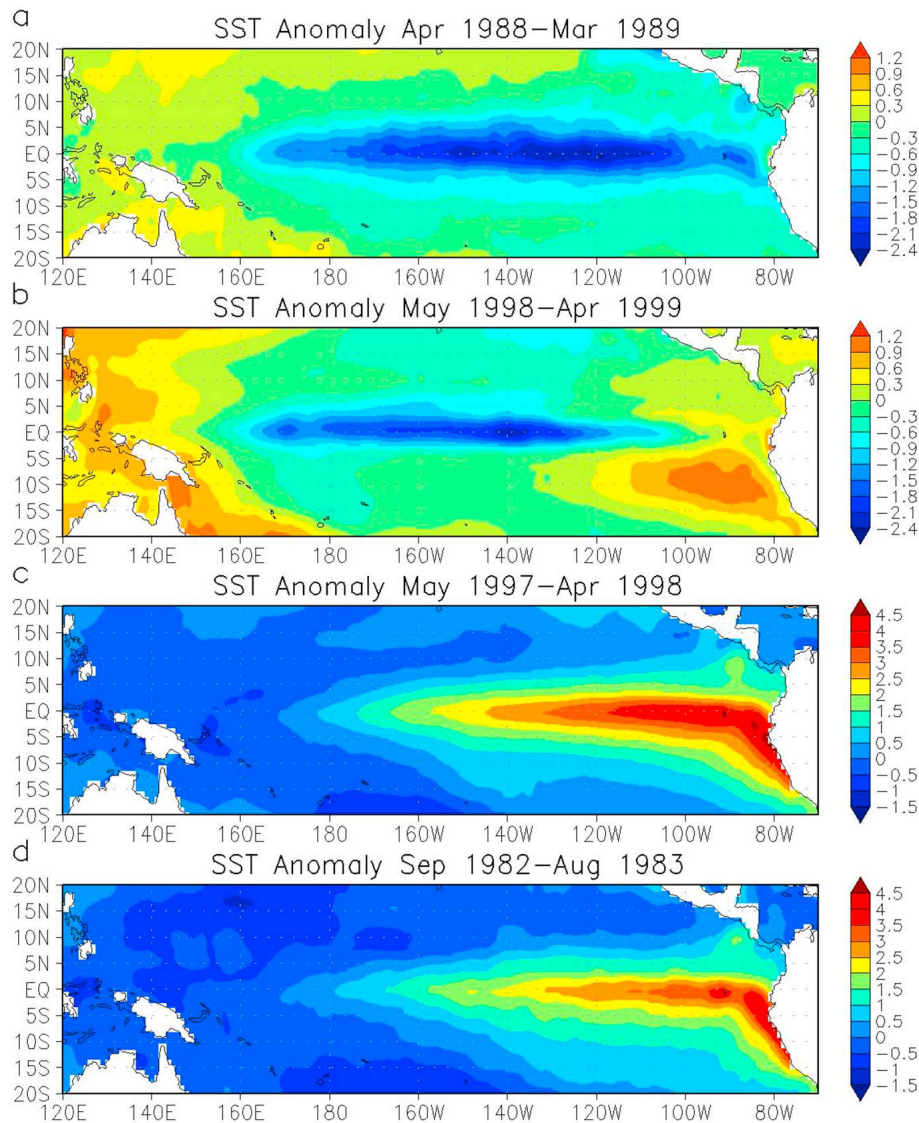


Figure 2. SST anomalies of ENSO over the period (a) April 1988 to March 1989, (b) May 1998 to April 1999, (c) May 1997 to April 1998, and (d) September 1982 to August 1983.

oceanic and atmospheric variability associated with ENSO in recent years. In particular, its spatial structure during ENSO cold events is emphasized by describing the inter-annual variation of anomalous surface currents in the tropics. We demonstrate that La Niña Modoki events can be clearly identified by the spatial pattern of surface currents based on these analyses. Also, anomalous circulations in the western Pacific near the coast of the Philippines associated with La Niña Modoki are discussed by comparing them with the surface winds and SST in the tropical Pacific.

2. Data

[6] We use six primary data sets in this study. Near-surface velocity data, derived from the Ocean Surface Current Analysis–Real time (OSCAR) project [Lagerloef *et al.*, 1999], are used to describe the spatial pattern of surface currents during El Niño and La Niña events. The OSCAR

velocities are estimated using sea surface height (SSH) data from satellite altimeter measurements, surface wind stress, and drifter data, and they are presented in the form of 5 day average near-surface velocity fields on a $1^\circ \times 1^\circ$ grid over the period January 1993 to July 2010. Interannual variations in SSH are identified using monthly multisatellite analyses of SSH anomalies over the period December 1992 to May 2009. These analyses are obtained from Archiving, Validation, and Interpretation of Satellite Oceanographic (AVISO) data. The SST anomalies associated with ENSO are described using the SST data from the Tropical Rainfall Measuring Mission Microwave Imager (TMI) for the period January 2002 to December 2008. The 3 day average TMI SST data were originally gridded at $0.25^\circ \times 0.25^\circ$, but we averaged the data onto a $1^\circ \times 1^\circ$ grid. Also, monthly SST data from the blended product of satellite/in situ observations [Reynolds *et al.*, 2002] are used to cover the period for which the TMI SST data are not available. The data were analyzed

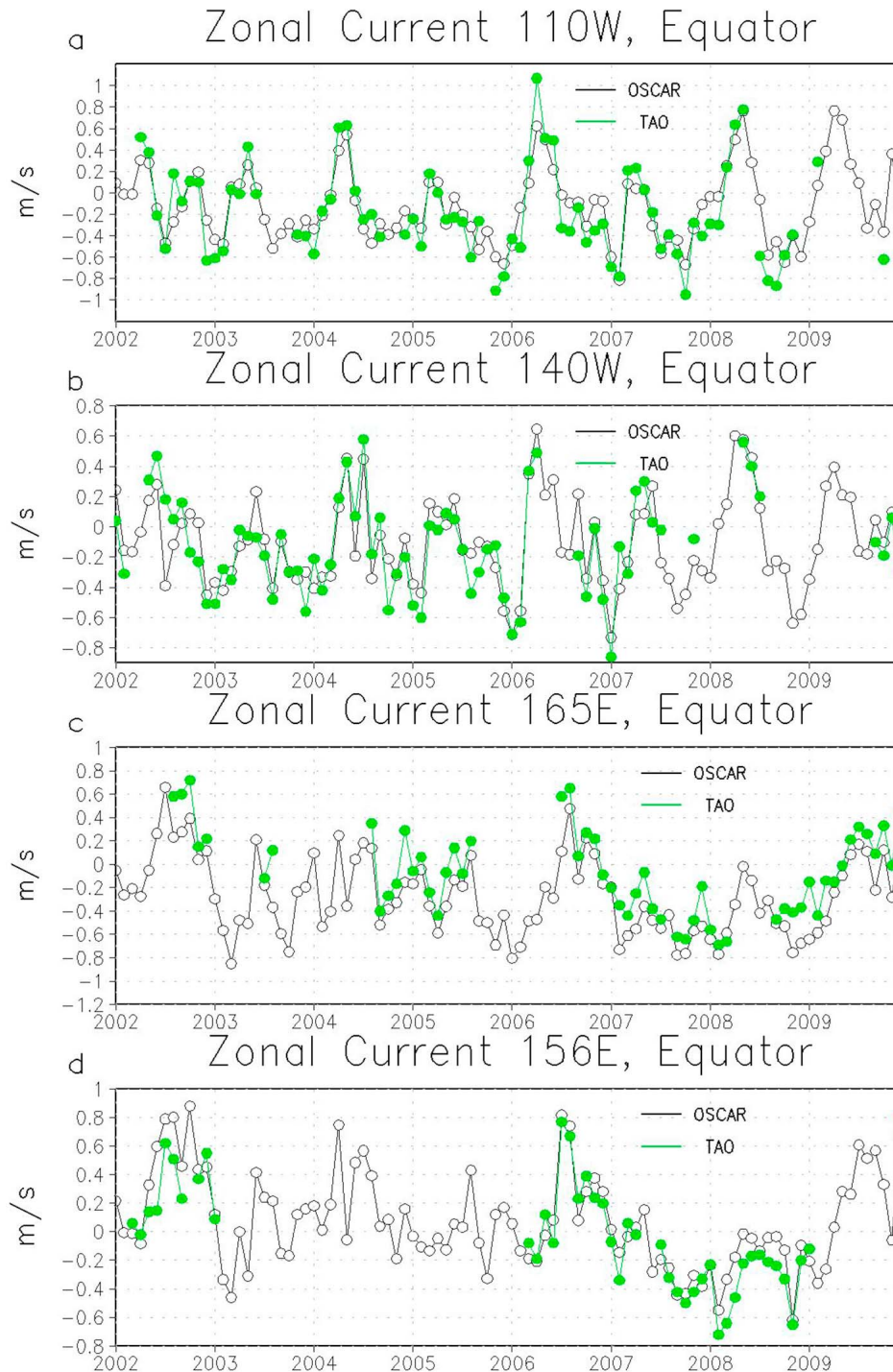


Figure 3. Time series of monthly zonal velocity on the equator at (a) 110°W, (b) 140°W, (c) 165°E, and (d) 156°E from OSCAR data (black lines) and from TAO moorings at 10 m (green lines).

over the 29 year period (December 1981 to December 2010) using 1° resolution. The anomalous surface winds associated with El Niño and La Niña are defined using 3 day average analyses of surface winds derived from the Quick Scatterometer (QSCAT; January 2000 to October 2009) [Tang and Liu, 1996]. Surface wind stress data from the National Centers for Environmental Prediction/Department of Energy

reanalysis [Kanamitsu *et al.*, 2002] are also used to describe the variation of the zonal wind stress associated with El Niño and La Niña.

[7] Since the OSCAR velocities are not derived from direct current measurements at each grid point, it is necessary to validate them by comparison with existing direct measurements, especially near the equator, where geostrophic

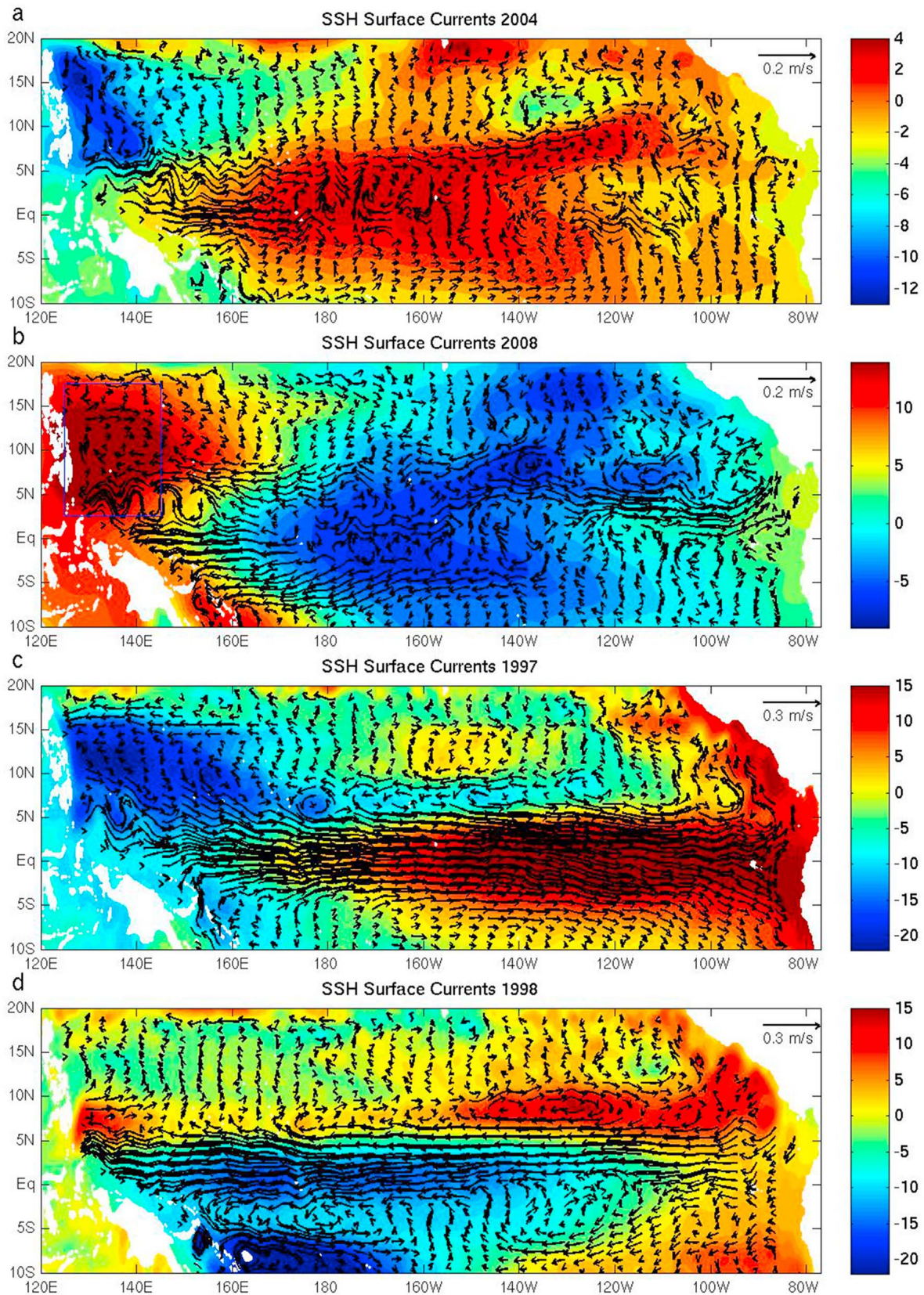


Figure 4. Average surface current (arrows) and SSH (color) anomalies during (a) 2004, (b) 2008, (c) 1997, and (d) 1998. The average period in Figures 4a–4d is the entire calendar year for each year.

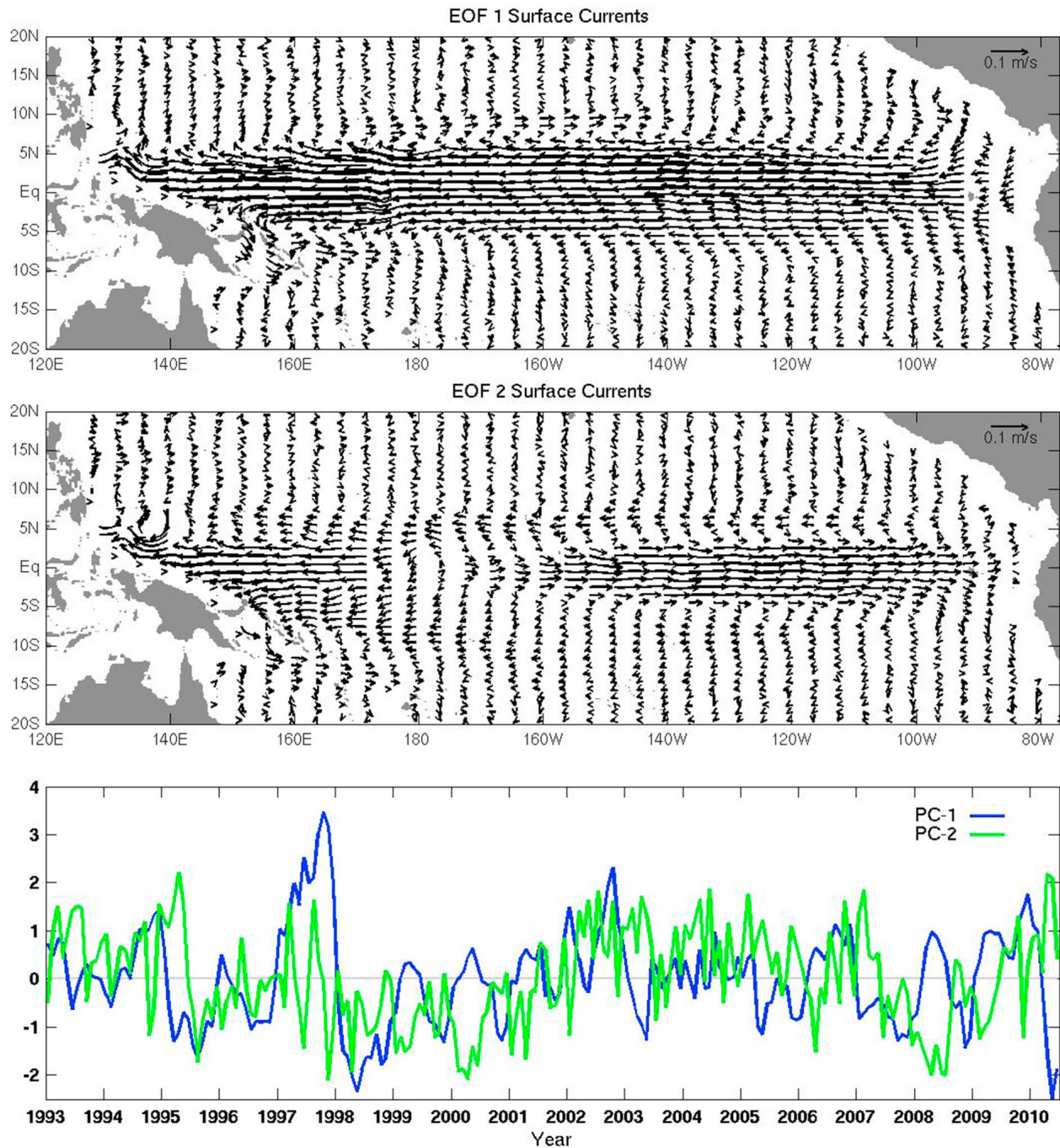


Figure 5. (top) First and (middle) second surface current eigenvectors for the domain (20°N–20°S, 120°E–70°W). The eigenvectors have been scaled for a one standard deviation anomaly of each principal component. (bottom) Time series of first and second principal components. The two leading EOFs capture 24.6% and 6.8% of the total variance, respectively.

balance does not necessarily hold. Previous studies have demonstrated that the zonal velocity from OSCAR near the equator agrees well with that from Tropical Ocean–Global Atmosphere Tropical Atmosphere–Ocean (TAO) buoys [McPhaden, 1995] on various time scales, including annual, interannual [Bonjean and Lagerloef, 2002], and subseasonal [Shinoda *et al.*, 2009]. Here we compare OSCAR zonal

velocities with the TAO data in the western and eastern Pacific during recent years. Figure 3 shows the surface zonal velocity from OSCAR and the zonal velocity at 10 m depth from four of the TAO moorings located on the equator. These comparisons of monthly mean time series show very good agreement in both the western and the eastern Pacific (correlation coefficient $r=0.90$ at 110°W, $r=0.85$ at 140°W,

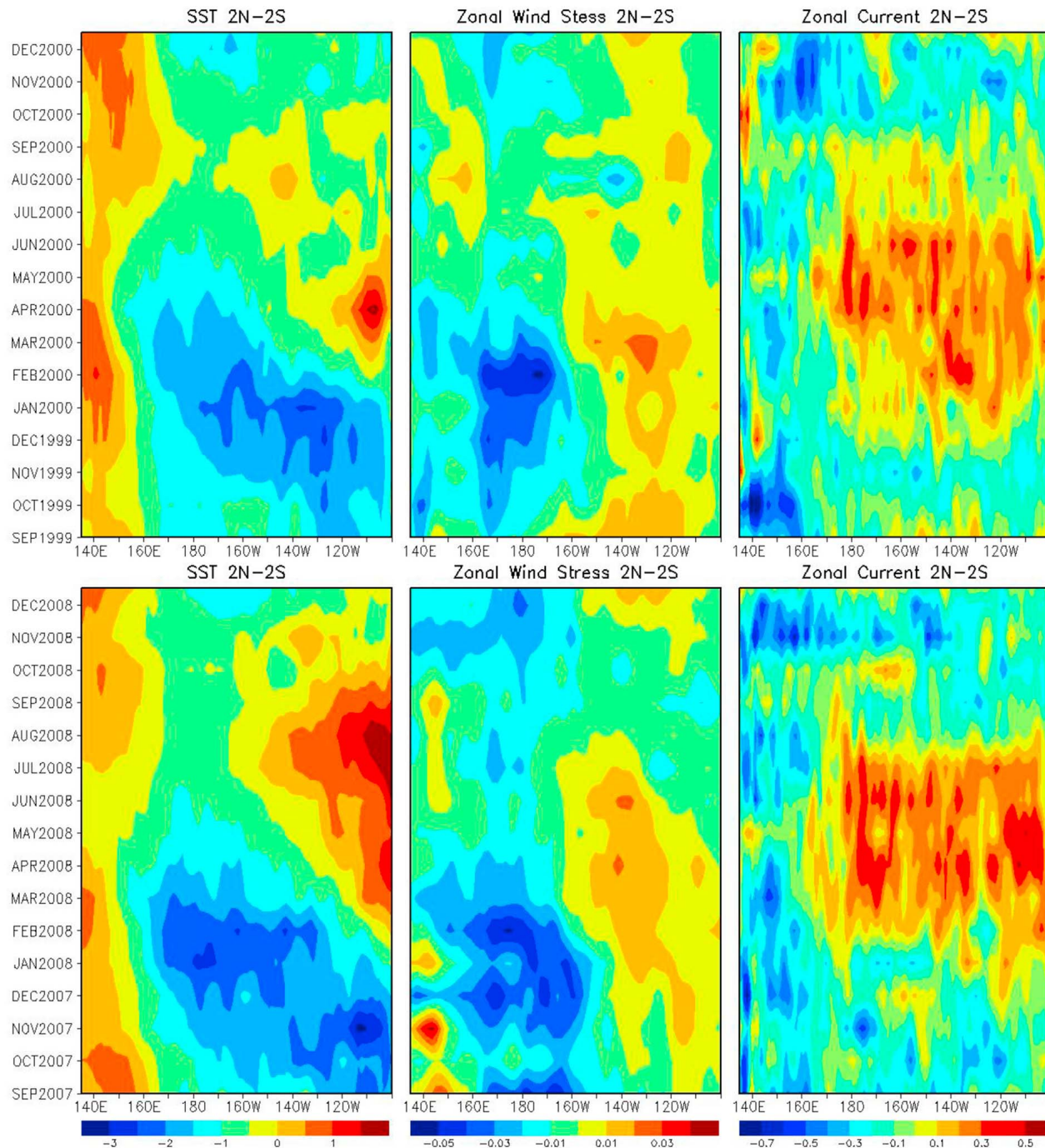


Figure 6. Longitude-time diagrams of monthly mean (left) SST, (middle) zonal wind stress, and (right) zonal current anomalies averaged over 2°N–2°S during (top) September 1999 to October 2000 and (bottom) September 2007 to October 2008. Anomalies are calculated by subtracting the annual cycle (first three harmonics of the seasonal cycle) for the period 1982–2010 (SST), 1979–2010 (wind stress), and 1993–2009 (zonal current).

$r = 0.94$ at 165°E, and $r = 0.93$ at 156°E). Therefore, we conclude that OSCAR velocity data are suitable for examining interannual variations of surface currents in the tropics, including their spatial patterns during El Niño and La Niña events.

[8] It should be noted that a recent study shows significant errors in OSCAR meridional velocities near the equator [Johnson *et al.*, 2007]. However, the surface current anomalies near the equator associated with El Niño and La Niña are predominantly zonal, and thus, the error in

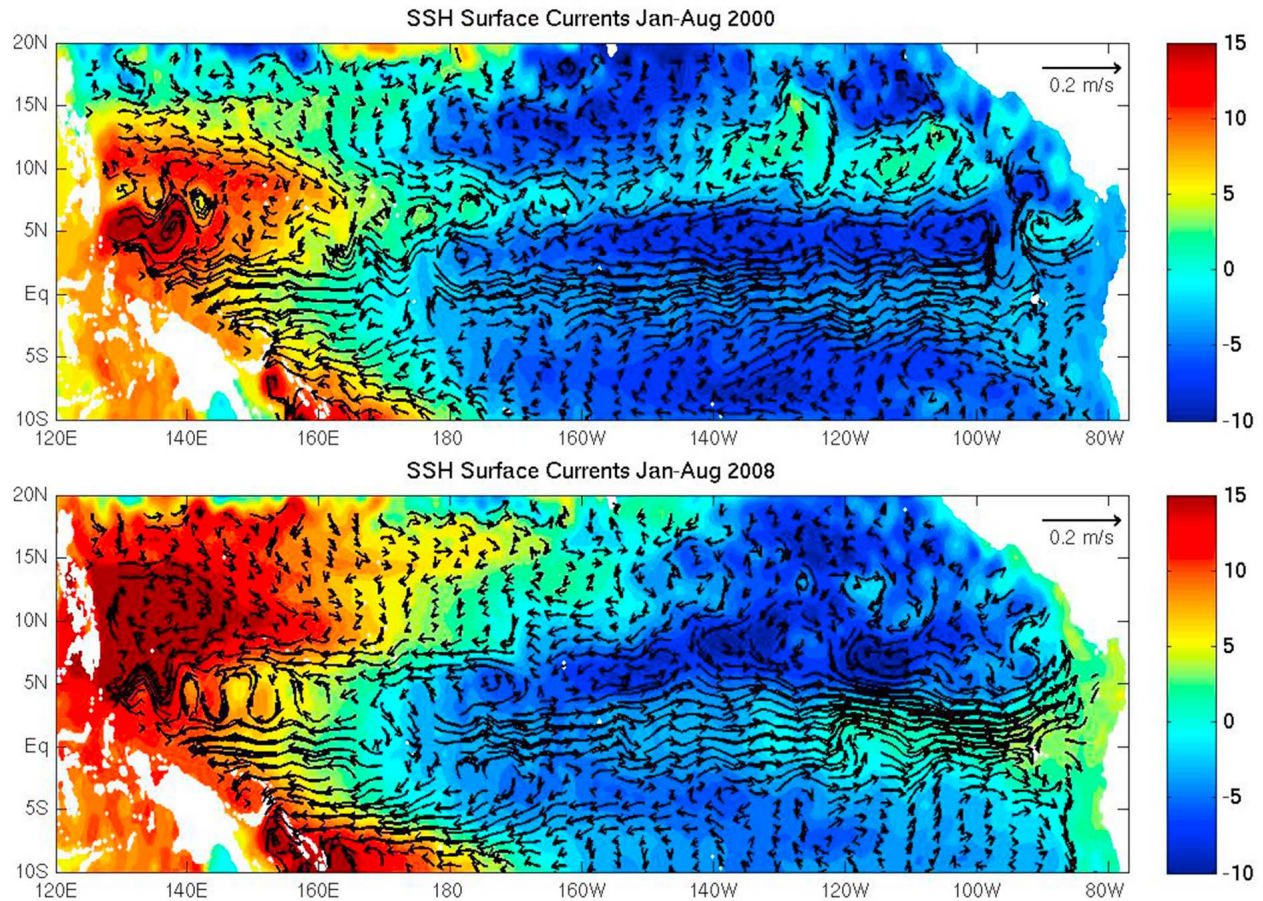


Figure 7. Same as Figure 4 except for the period (top) January–August 2000 and (bottom) January–August 2008.

meridional velocity should not significantly impact the results of analyses discussed in this study.

3. Results

[9] During the 2004 El Niño Modoki event, strong anomalous surface currents associated with SSH anomalies in the tropical ocean were observed (Figure 4). The surface current anomalies in the equatorial Pacific show convergence, with eastward currents west of the dateline and westward currents east of it. In the western Pacific around 5°N – 15°N , an anomalous cyclonic circulation associated with a negative SSH anomaly is observed. The anomalous circulation pattern during 2008 is nearly the opposite of 2004 in that the equatorial currents show divergence, and an anomalous anticyclonic circulation is found in the western Pacific north of the equator (Figure 4b, see also Figure 6). These equatorial circulation patterns during 2004 and 2008 are clearly different from those observed during the strong El Niño event in 1997 and the subsequent La Niña event in 1998 (Figures 4c and 4d). The anomalous currents are eastward (westward) in the entire equatorial Pacific during 1997 (1998).

[10] Spatial patterns of anomalous currents, similar to those in ENSO and ENSO Modoki years as shown in

Figure 4, are found in the first two empirical orthogonal functions (EOFs) of the surface currents (Figure 5). The first EOF depicts an equatorial current anomaly that is quite uniform across the entire Pacific, whereas the second EOF depicts a region of convergence (divergence) in the equatorial zonal current anomaly just east of the dateline.

[11] During 2000 and 2008, the principal component of the second EOF (PC-2) is much lower than average, while that of the first EOF (PC-1) is near normal. The contrast between the two PCs is particularly large in 2008. The evolution of SST, zonal wind stress, and zonal current anomalies near the equator (2°N – 2°S) during these years (Figure 6) demonstrate similar evolution during each event. The coldest SST anomalies near the equator are found east of 140°W in late 1999 and 2007. These cold anomalies propagate westward and are flanked by warm anomalies during northern spring and summer of 2000 and 2008. During each year, divergence of the zonal wind is observed. Strong anomalous eastward currents associated with these SST and wind anomalies are generated during January–August. The spatial structure of the mean surface currents during these periods shows more prominent divergence of equatorial zonal currents near the dateline (Figure 7). These analyses provide a basis for classifying 2000 and 2008 as periods with La Niña Modoki events that are the counterpart

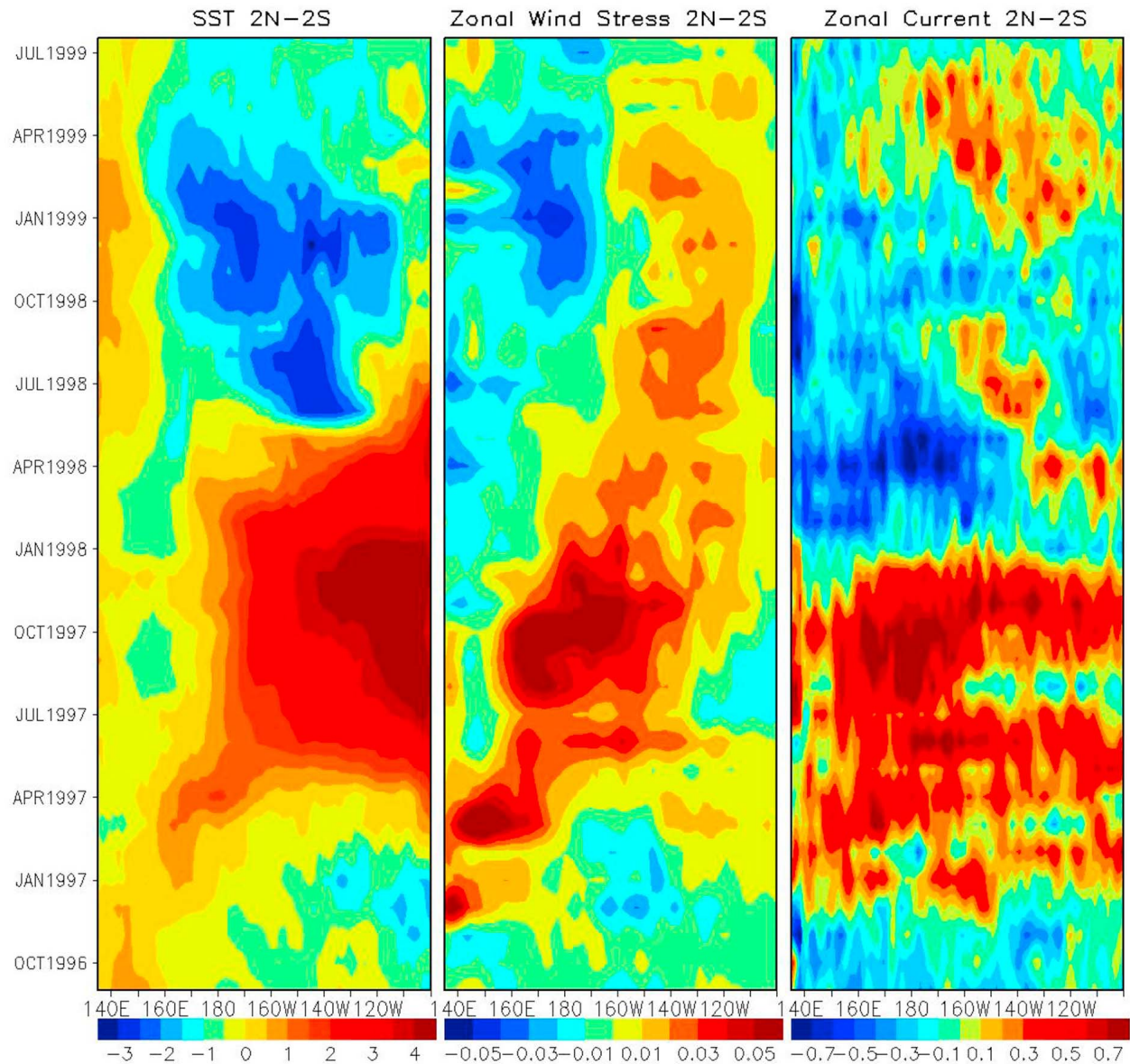


Figure 8. Same as Figure 6 except for the period September 1996 to July 1999.

of El Niño Modoki events, such as that occurred in 2004. A similar pattern of surface currents occurred during early 1999, but the current anomalies were weaker and the event lasted for a shorter period (~5 months).

[12] To compare the evolution of La Niña Modoki with that of traditional La Niña and El Niño, variations of SST, zonal wind stress, and zonal current near the equator during the 1997 El Niño and subsequent 1998 La Niña are examined (Figure 8). The onset of 1998 La Niña and the termination of 1997 El Niño occur during May 1998, as evident in the sudden change of SST anomalies during this period. However, the quick reversal of zonal current anomalies in the entire equatorial Pacific is observed in December 1997, which is 5 months before the onset of La Niña based on the SST anomaly. The westward current anomalies prevail throughout the calendar year although occasional short

periods of eastward current anomalies are found in the eastern Pacific during the first half of 1998 [Picaut *et al.*, 2002]. However, the zonal extent of these anomalous eastward currents is much smaller than those associated with La Niña Modoki. This short time scale variability may be caused by intraseasonal variations in surface winds, associated with the Madden-Julian Oscillation (MJO) [Madden and Julian, 1971], observed during this period [Takayabu *et al.*, 1999].

[13] A reversal of zonal currents, similar to that in December 1997, is also evident before the onset of the 1997 El Niño. On the basis of the evolution of SST anomalies, the onset occurs around May 1997. However, the quick reversal of zonal currents across the entire equatorial Pacific is found in December 1996, and anomalous eastward currents are observed throughout 1997. These variations in equatorial

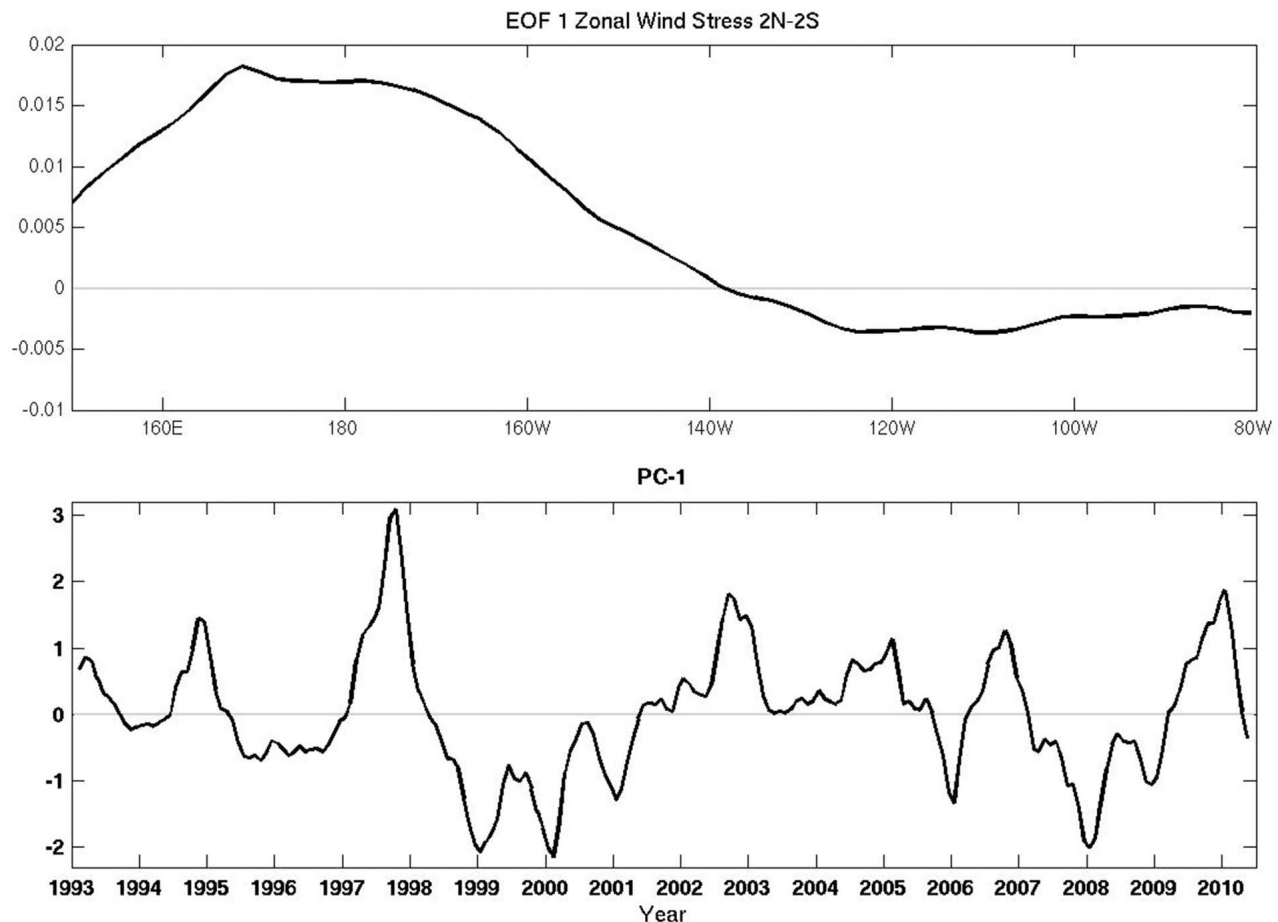


Figure 9. (top) First eigenvector of surface zonal wind stress (N m^{-2}) averaged over 2°N – 2°S for the domain 150°E – 80°W . The eigenvector has been scaled for a one standard deviation anomaly of the principal component. The leading EOF captures 55.6% of the total variance. (bottom) Time series of the first principal component. A 1-2-1 smoothing was applied to the monthly time series.

zonal current suggest that real-time monitoring of the spatial pattern of velocity fields may help predict the onset, development, and termination of ENSO warm and cold events.

[14] The 1998 La Niña event is followed by a weak La Niña Modoki event in 1999, which is shown in the time series of PC-1 and PC-2 (Figure 3). The divergent pattern of zonal currents is generated in January 1999 (Figure 8). Prior to the change of the current pattern, a strong divergence of zonal winds develops during late 1998 to early 1999 (Figure 8). The strong easterly anomalies centered at around 160°E – 180°E are associated with weaker westerly anomalies in the eastern Pacific at around 160°W – 120°W . This wind pattern is quite similar to that during 2000 and 2008 (Figure 6). The distinct difference in zonal wind pattern between 1998 La Niña and 1999 La Niña Modoki events suggests that the divergent pattern of zonal currents during the La Niña Modoki events are generated by equatorial zonal winds with a strong basin-scale divergence in the Pacific.

[15] The strong divergence of zonal wind anomaly during La Niña Modoki events is further demonstrated by the EOF analysis of surface zonal wind stress near the equator (Figure 9). The spatial pattern of the first EOF, which shows

convergence/divergence, is quite similar to the zonal wind stress pattern observed prior to and during La Niña Modoki (Figures 6, 8, and 9). The time series of PC-1 indicate that the divergence of zonal winds is exceptionally strong during early 1999, 2000, and 2008, which is followed by the divergent zonal current pattern. This suggests that the anomalous zonal current pattern is directly driven by equatorial winds during La Niña Modoki events. However, the equatorial current pattern during the 1998 La Niña event, which is westward throughout the entire basin, cannot be explained as a simple linear response to local winds during this period. A variety of other processes could be involved in generating upper ocean variability associated with traditional La Niña, and thus, the effect of the surface wind forcing is not necessarily visible in the spatial and temporal variations of zonal currents.

[16] Figure 10 demonstrates the opposite spatial pattern of the surface wind anomaly during 2004 and 2008. A strong convergence (divergence) of surface winds in the equatorial region and a cyclonic (anticyclonic) wind pattern in the western Pacific north of the equator are evident in 2004 (2008). Ekman pumping velocity anomalies in the western Pacific around 10°N are consistent with the SSH

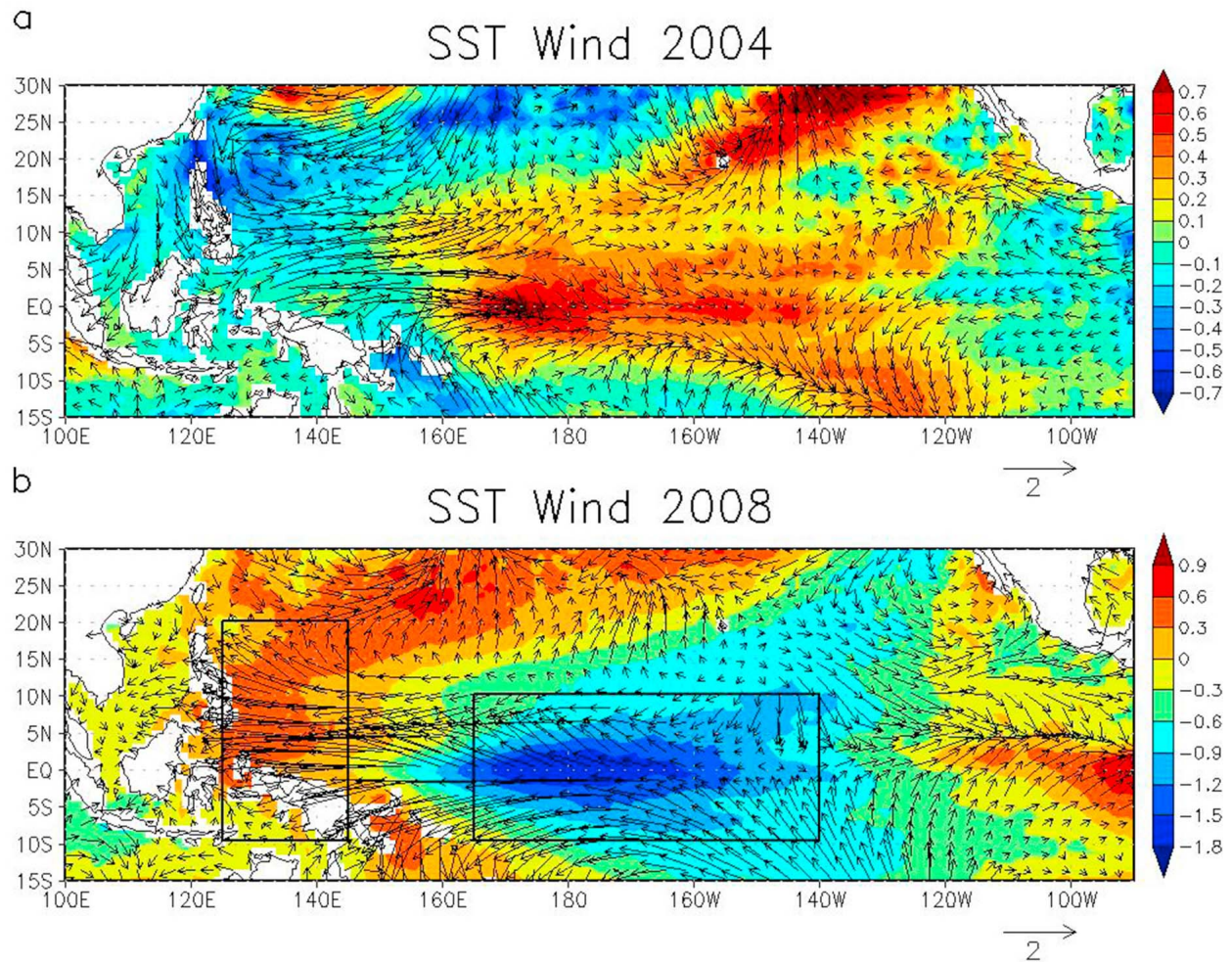


Figure 10. Yearly mean SST and surface wind (arrows) anomalies for (a) 2004 and (b) 2008. The rectangles in Figure 10b are the areas used to calculate EMI2 (see text for the definition).

and circulation anomalies east of the Philippines (Figure 11). This suggests that surface wind anomalies associated with anomalous SSTs in the tropical western and central Pacific generate cyclonic and anticyclonic ocean circulation anomalies in the western Pacific north of the equator through the changes in wind stress curl. This anomalous wind stress curl further impacts anomalous currents through Straits west of the Philippines, as SSH anomalies east of the Philippines are generally associated with circulation anomalies in the Philippine Archipelago [Metzger and Hurlburt, 1996; Hurlburt *et al.*, 2011]. A previous modeling study suggests that remotely forced Rossby waves may also influence interannual SSH variability in this region during ENSO events in addition to local wind forcing [Tozuka *et al.*, 2002]. Further modeling studies are necessary to identify the contributions of remote forcing to the SSH variations during ENSO Modoki.

[17] To confirm the air-sea interaction processes described previously, we define a new index that represents the SST gradient in the western and central Pacific. The EMI [Ashok *et al.*, 2007] is defined as

$$\text{EMI} = [\text{SST}]_A - 0.5[\text{SST}]_B - 0.5[\text{SST}]_C,$$

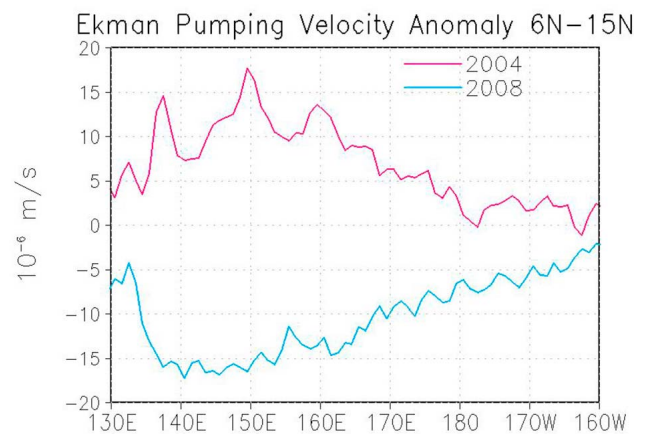


Figure 11. Ekman pumping velocity anomaly averaged over 6°N–15°N in 2004 (red line) and 2008 (blue line). QSCAT winds are used to calculate the Ekman pumping velocity.

Table 1. Correlation Coefficients Between SSH Anomalies in the Western Pacific (125°E–145°E, 2.5°N–17.5°N), EMI2, EMI, and Niño3 SST Anomaly

	Correlation Coefficient
West Pacific SSH versus EMI2	0.88
West Pacific SSH versus Niño3 SST	0.71
West Pacific SSH versus EMI	0.66
Niño3 SST versus EMI2	0.67
Niño3 SST versus EMI	0.19

where $[SST]_A$, $[SST]_B$, and $[SST]_C$ are the average SST anomalies over regions A (165°E–140°W, 10°S–10°N), B (110°W–70°W, 15°S–5°N), and C (125°E–145°E, 10°S–20°N), respectively. Here the new index, EMI2, is defined as

$$EMI2 = [SST]_A - 0.5[SST]_C,$$

where the second term, which represents the contribution of anomalous SST in the eastern Pacific, is removed from EMI. EMI2 is well correlated with the western Pacific SSH anomaly ($r = 0.88$), indicating that the anomalous circulation east of the Philippines is strongly related to the SST gradient in the western and central Pacific. As Niño3 SST is relatively well correlated with EMI2, the western Pacific SSH anomaly is significantly correlated with Niño3 SST as well (Table 1). However, EMI2 is much lower than the average, and the western Pacific SSH anomalies show large positive values during the strong La Niña Modoki event in 2008, while Niño3 SST is near normal most of the time during the event. EMI is well correlated with the western Pacific SSH after 2000 (Figure 12), but EMI is normal during the 1997 El Niño event because of the stronger warming in the eastern Pacific as well as a large SST gradient in the western and central Pacific. This suggests that the SST anomaly in the eastern Pacific does not have a direct influence on the circulation in the western Pacific north of the equator.

4. Discussion

[18] While the analysis demonstrates the important role of equatorial surface wind forcing in generating the divergent pattern of zonal current anomaly during La Niña Modoki events, the current pattern during a traditional La Niña event cannot be well explained as a direct response to local winds. For example, a quick reversal of equatorial zonal current anomaly across the entire equatorial Pacific occurs in late 1997, an event followed by the transition from a traditional El Niño to La Niña 5 months later. However, the zonal winds do not show such a reversal during this period. The mechanism of transition between the ENSO warm and cold events is suggested by many previous studies [e.g., Schopf and Suarez, 1988; Weisberg and Wang, 1997; Picaut *et al.*, 1997; Jin, 1997; Wang, 2001; Kessler, 2002] (see also Wang and Picaut [2004] and Chang *et al.* [2006] for reviews). A variety of oceanic and atmospheric processes such as the changes of Sverdrup transport due to off-equatorial winds [Jin, 1997] and the propagation and reflection of equatorial waves [Schopf and Suarez, 1988; Picaut *et al.*, 1997] are involved in some of these ENSO theories. Accordingly, upper ocean current variations associated with ENSO and ENSO Modoki events may be determined by a

combination of different equatorial and off-equatorial oceanic and atmospheric processes. However, most previous theories focus mainly on explaining SST, thermocline depth, and wind variations associated with ENSO, and the basin-scale variation of upper ocean currents is not a major component of the theories. Further observational and modeling studies that focus on processes directly relevant to the surface current variations are needed to fully establish the theory of ENSO and ENSO Modoki.

[19] The analyses indicate that strong anticyclonic (cyclonic) circulation anomalies in the western Pacific east of Philippines are evident during La Niña (El Niño) Modoki. These circulation anomalies off the Philippines could

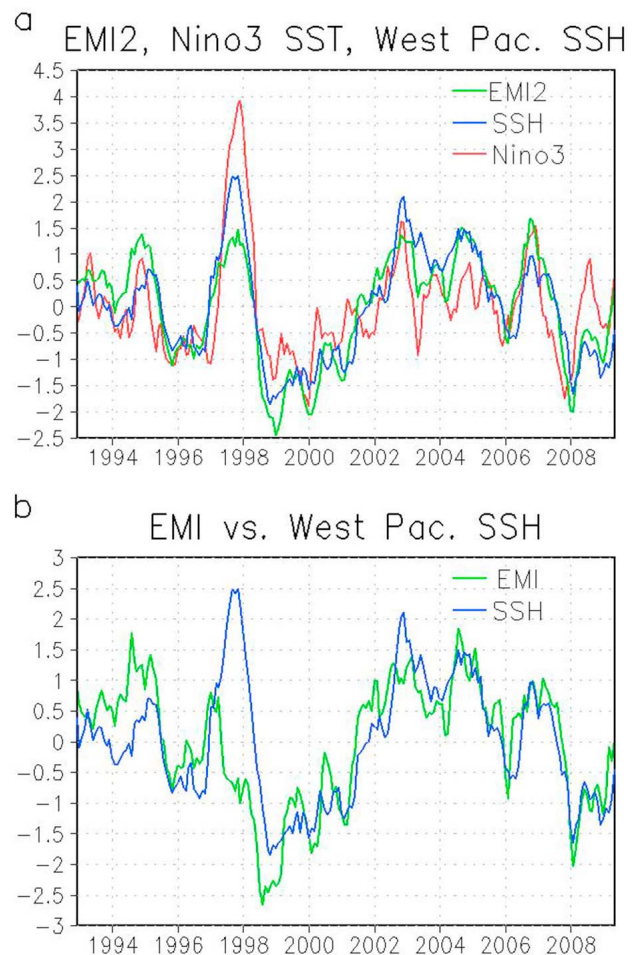


Figure 12. (a) Time series of EMI2 (green line, see text for the definition), SSH anomalies (blue line) averaged over 125°E–145°E, 2.5°N–17.5°N (rectangle in Figure 1b), and Niño3 (150°W–90°W, 5°N–5°S) SST anomalies (red line). Time series are normalized by their standard deviations, and linear trends are removed. The sign of the SSH anomalies is changed for the comparison. (b) Time series of EMI (green line, see text for the definition) and SSH (blue line) anomalies averaged over 125°E–145°E and 2.5°N–17.5°N (the rectangle in Figure 1b). Time series are normalized by their standard deviations, and linear trends are removed. The sign of the SSH anomalies is changed for the comparison.

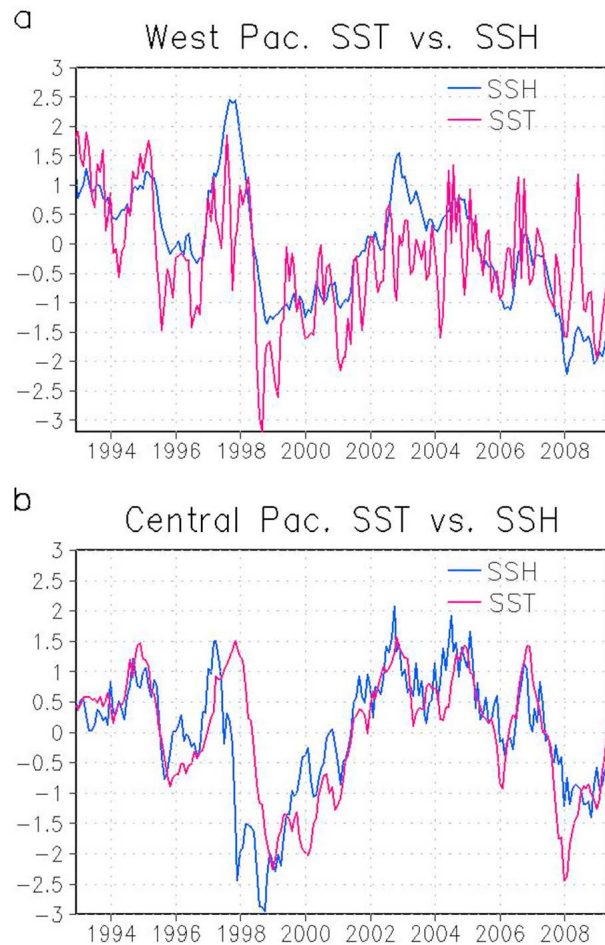


Figure 13. (a) Time series of SSH (blue line) and SST (red line) anomalies averaged over 125°E – 145°E and 2.5°N – 17.5°N (the rectangle in Figure 1b). Time series are normalized by their standard deviations. The sign of SSH and SST is changed for the consistency with Figure 12. (b) Same as Figure 13a except for the area 165°E – 140°W and 10°S – 10°N , and the sign of the anomalies is not changed.

influence SST in the western Pacific, which in turn may affect the atmospheric circulation. Here we further discuss the possible feedback mechanisms associated with La Niña Modoki. Figure 13a shows time series of SSH and SST anomalies east of the Philippines. The SST is significantly correlated with SSH ($r = 0.66$), suggesting that the circulation anomalies and the associated anomalous upper ocean structure could influence the SST in this region. A deeper thermocline associated with the anticyclonic circulation during La Niña Modoki events tends to generate warmer SST anomalies. The weakening of the Mindanao Current may also contribute to the anomalously warm SST. The SST anomaly in the central equatorial Pacific is also significantly correlated with the SSH anomaly (Figure 13b; $r = 0.68$), suggesting that anomalous easterlies in this region during La Niña Modoki may enhance SST cooling through the equatorial upwelling [Ashok *et al.*, 2007]. The increase of SST off the Philippines and the decrease of SST in the central

Pacific through oceanic processes then result in the larger SST difference between the western and central Pacific. The large SST gradient could further enhance the atmospheric circulation, which is associated with the negative wind stress curl anomalies around 10°N in the western Pacific. The anticyclonic ocean circulation then becomes stronger due to the wind stress curl, and thus, these processes could provide a positive feedback mechanism in the western and central Pacific.

[20] These air-sea feedback mechanisms may be affected by a variety of oceanic and atmospheric processes during different time periods. Although SST and SSH off the Philippines are moderately correlated, the circulation anomalies do not always seem to have a significant impact on SST. For example, the SST in this region is near normal during 2003, while the SSH anomaly is negative in association with the anomalous cyclonic circulation (Figure 13a). These discrepancies suggest an influence by other factors, including shorter time scale variability such as the MJO and interaction with the seasonal cycle.

[21] A number of processes could also be involved in the generation of anomalous wind stress curl in the western Pacific [e.g., Zhang *et al.*, 1996; Wang and Zhang, 2002; Feng *et al.*, 2010]. The sea level pressure gradient associated with the SST gradient during La Niña Modoki may initially drive southeasterly winds in the western Pacific north of the equator [e.g., Lindzen and Nigam, 1987]. Changes of diabatic heating associated with SST anomalies could also induce similar wind anomalies [e.g., Gill, 1980; Zhang and Krishnamurti, 1996]. These winds could be influenced by the land topography of the Philippine Archipelago and convection around the Maritime Continent. Also, winds and SST at higher latitudes may affect the anomalous anticyclonic atmospheric circulation through tropical-extratropical interaction. A thorough investigation of oceanic, atmospheric, and land processes and their interactions in this region is thus needed to fully understand the feedback mechanisms associated with ENSO Modoki.

5. Summary

[22] During ENSO cold events (La Niña), a prominent cooling of SST is generally observed in the central equatorial Pacific, while the maximum SST anomaly is observed near the eastern boundary during ENSO warm events (El Niño). Because of this asymmetry in the SST anomaly pattern between the warm and cold events, it is difficult to clearly distinguish the two types of La Niña from the spatial pattern of SST. In this study, we have distinguished La Niña Modoki events, like those that occurred in 2000 and 2008, from other La Niña events by using surface current data. During La Niña Modoki events, a divergence of zonal currents in the equatorial Pacific is observed near the dateline, which is opposite to surface current anomalies during El Niño Modoki events (e.g., the 2004 event). Thus, unlike canonical El Niño/La Niña, the spatial pattern of both surface currents and SST is antisymmetric for El Niño/La Niña Modoki. For traditional El Niño/La Niña, the surface current anomaly pattern is antisymmetric, and is characterized by eastward/westward current anomalies across the entire tropical Pacific, while the SST anomaly pattern exhibits the asymmetry described previously.

[23] Anomalous circulations east of the Philippines are associated with the anomalous SST gradient in the central and western tropical Pacific and wind stress curl in the western Pacific. A strong SST gradient, associated with a cold anomaly in the central Pacific, is generally observed during both La Niña and La Niña Modoki events and can generate negative wind stress curl anomalies in the western tropical Pacific north of the equator. Hence, the anomalous anticyclonic circulation near the coast of the Philippines, which is associated with the strong SST gradient in the central and western Pacific, is observed during the 2008 La Niña Modoki event even though Niño3 SST is near normal.

[24] Because of the limited (19 year) record of satellite altimeter data, we could currently identify only three La Niña Modoki events based on the spatial pattern of surface currents. Yet these analyses demonstrate that the 1999, 2000, and 2008 cold events are clearly different from other La Niña events. Although much longer SST records are available, significant cold SST anomalies in the central Pacific near the dateline are found during both types of cold events, and thus, both canonical El Niño (e.g., Niño3.4 SST) and El Niño Modoki (EMI) indices are not effective in distinguishing between them. Our results suggest that surface currents during La Niña would be useful in efforts to examine changes in the characteristics of cold events in recent years. A longer time series is needed for future reanalysis of the results in this study.

[25] **Acknowledgments.** We acknowledge the OSCAR Project Office for making the surface velocity data available. The altimeter products are produced by SSALTO/DUACS and are distributed by AVISO. The TMI SST and QuikScat wind data are produced by Remote Sensing Systems. The TAO project office of NOAA/PMEL provided the mooring time series data. This research is supported in part by three 6.1 projects including Global Remote Littoral Forcing via Deep Water Pathways (program element 601153N) and a 6.2 project Full Column Mixing for Numerical Ocean Models (program element 602435N) sponsored by the Office of Naval Research and by the NOAA Modeling, Analysis, Predictions and Projections (MAPP) Program.

References

- Alexander, M. A., I. Bladé, M. Newman, J. R. Lanzante, N.-C. Lau, and J. D. Scott (2002), The atmospheric bridge: The influence of ENSO teleconnections on air–sea interaction over the global oceans, *J. Clim.*, *15*, 2205–2231, doi:10.1175/1520-0442(2002)015<2205:TABTIO>2.0.CO;2.
- Ashok, K., S. K. Behera, S. A. Rao, H. Weng, and T. Yamagata (2007), El Niño Modoki and its possible teleconnection, *J. Geophys. Res.*, *112*, C11007, doi:10.1029/2006JC003798.
- Bonjean, F., and G. S. E. Lagerloef (2002), Diagnostic model and analysis of the surface currents in the tropical Pacific Ocean, *J. Phys. Oceanogr.*, *32*, 2938–2954, doi:10.1175/1520-0485(2002)032<2938:DMAAOT>2.0.CO;2.
- Chang, P., et al. (2006), Climate fluctuations of tropical coupled systems—The role of ocean dynamics, *J. Clim.*, *19*, 5122–5174, doi:10.1175/JCLI3903.1.
- Feng, J., L. Wang, W. Chen, S. Fong, and K. Leong (2010), Different impacts of two types of Pacific Ocean warming on Southeast Asian rainfall during boreal winter, *J. Geophys. Res.*, *115*, D24122, doi:10.1029/2010JD014761.
- Gill, A. E. (1980), Some simple solutions for heat-induced tropical circulation, *Q. J. R. Meteorol. Soc.*, *106*, 447–462, doi:10.1002/qj.49710644905.
- Hoerling, M. P., A. Kumar, and M. Zhong (1997), El Niño, La Niña, and the nonlinearity of their teleconnections, *J. Clim.*, *10*, 1769–1786, doi:10.1175/1520-0442(1997)010<1769:ENOLNA>2.0.CO;2.
- Horel, J. D., and J. M. Wallace (1981), Planetary-scale atmospheric phenomena associated with the Southern Oscillation, *Mon. Weather Rev.*, *109*, 813–829, doi:10.1175/1520-0493(1981)109<0813:PSAPAW>2.0.CO;2.
- Hurlburt, H. E., E. J. Metzger, J. Sprintall, S. N. Riedlinger, R. A. Arnone, T. Shinoda, and X. Xu (2011), Circulation in the Philippine Archipelago simulated by 1/12° and 1/25° global HYCOM and EAS NCOM, *Oceanography*, *24*(1), 28–47, doi:10.5670/oceanog.2011.02.
- Jin, F.-F. (1997), An equatorial ocean recharge paradigm for ENSO. Part I: Conceptual model, *J. Atmos. Sci.*, *54*, 811–829, doi:10.1175/1520-0469(1997)054<0811:AEORPF>2.0.CO;2.
- Johnson, E. S., F. Bonjean, G. S. E. Lagerloef, and J. T. Gunn (2007), Validation and error analysis of OSCAR sea surface currents, *J. Atmos. Oceanic Technol.*, *24*, 688–701, doi:10.1175/JTECH1971.1.
- Kanamitsu, M., W. Ebisuzaki, J. Woollen, S.-K. Yang, J. J. Hnilo, M. Fiorino, and G. L. Potter (2002), NCEP-DOE AMIP-II reanalysis (R-2), *Bull. Am. Meteorol. Soc.*, *83*, 1631–1643, doi:10.1175/BAMS-83-11-1631.
- Kao, H.-Y., and J.-Y. Yu (2009), Contrasting eastern-Pacific and central-Pacific types of ENSO, *J. Clim.*, *22*, 615–632, doi:10.1175/2008JCLI2309.1.
- Kessler, W. S. (2002), Is ENSO a cycle or a series of events?, *Geophys. Res. Lett.*, *29*(23), 2125, doi:10.1029/2002GL015924.
- Kug, J.-S., F.-F. Jin, and S.-I. An (2009), Two types of El Niño events: Cold tongue El Niño and warm pool El Niño, *J. Clim.*, *22*, 1499–1515, doi:10.1175/2008JCLI2624.1.
- Kumar, K. K., B. Rajagopalan, M. Hoerling, G. Bates, and M. Cane (2006), Unraveling the mystery of Indian monsoon failure during El Niño, *Science*, *314*, 115–119, doi:10.1126/science.1131152.
- Lagerloef, G. S. E., G. T. Mitchum, R. Lukas, and P. P. Niiler (1999), Tropical Pacific near surface currents estimated from altimeter, wind, and drifter data, *J. Geophys. Res.*, *104*, 23,313–23,326, doi:10.1029/1999JC900197.
- Larkin, N. K., and D. E. Harrison (2002), ENSO warm (El Niño) and cold (La Niña) event life cycles: Ocean surface anomaly patterns, their symmetries, asymmetries, and implications, *J. Clim.*, *15*, 1118–1140, doi:10.1175/1520-0442(2002)015<1118:EWENO>2.0.CO;2.
- Larkin, N. K., and D. E. Harrison (2005), On the definition of El Niño and associated seasonal average U.S. weather anomalies, *Geophys. Res. Lett.*, *32*, L13705, doi:10.1029/2005GL022738.
- Lindzen, R. S., and S. Nigam (1987), On the role of sea surface temperature gradients in forcing low level winds and convergence in the tropics, *J. Atmos. Sci.*, *44*, 2418–2436, doi:10.1175/1520-0469(1987)044<2418:OTROSS>2.0.CO;2.
- Madden, R. A., and P. R. Julian (1971), Detection of a 40–50 day oscillation in the zonal wind in the tropical Pacific, *J. Atmos. Sci.*, *28*, 702–708, doi:10.1175/1520-0469(1971)028<0702:DOADOI>2.0.CO;2.
- McPhaden, M. J. (1995), The tropical atmosphere ocean array is completed, *Bull. Am. Meteorol. Soc.*, *76*, 739–741.
- McPhaden, M. J., and X. Zhang (2009), Asymmetry in zonal phase propagation of ENSO sea surface temperature anomalies, *Geophys. Res. Lett.*, *36*, L13703, doi:10.1029/2009GL038774.
- Metzger, E. J., and H. E. Hurlburt (1996), Coupled dynamics of the South China Sea, the Sulu Sea, and the Pacific Ocean, *J. Geophys. Res.*, *101*, 12,331–12,352, doi:10.1029/95JC03861.
- Philander, S. G. H. (1983), El Niño Southern Oscillation phenomena, *Nature*, *302*, 295–301, doi:10.1038/302295a0.
- Philander, S. G. H. (1985), El Niño and La Niña, *J. Atmos. Sci.*, *42*, 2652–2662, doi:10.1175/1520-0469(1985)042<2652:ENALN>2.0.CO;2.
- Picaut, J., F. Masia, and Y. duPenhoat (1997), An advective-reflective conceptual model for the oscillatory nature of the ENSO, *Science*, *277*, 663–666, doi:10.1126/science.277.5326.663.
- Picaut, J., E. Hackert, A. J. Busalacchi, R. Murtugudde, and G. S. E. Lagerloef (2002), Mechanisms of the 1997–1998 El Niño–La Niña, as inferred from space-based observations, *J. Geophys. Res.*, *107*(C5), 3037, doi:10.1029/2001JC000850.
- Rasmusson, E. M., and T. H. Carpenter (1982), Variations in tropical sea surface temperature and surface wind fields associated with the Southern Oscillation/El Niño, *Mon. Weather Rev.*, *110*, 354–384, doi:10.1175/1520-0493(1982)110<0354:VITSST>2.0.CO;2.
- Reynolds, R. W., N. A. Rayner, T. M. Smith, D. C. Stokes, and W. Wang (2002), An improved in situ and satellite SST analysis for climate, *J. Clim.*, *15*, 1609–1625, doi:10.1175/1520-0442(2002)015<1609:AII-SAS>2.0.CO;2.
- Ropelewski, C. F., and M. S. Halpert (1987), Global and regional scale precipitation patterns associated with the El Niño/Southern Oscillation (ENSO), *Mon. Weather Rev.*, *115*, 1606–1626, doi:10.1175/1520-0493(1987)115<1606:GARSPP>2.0.CO;2.
- Schopf, P. S., and M. J. Suarez (1988), Vacillations in a coupled ocean-atmosphere model, *J. Atmos. Sci.*, *45*, 549–566, doi:10.1175/1520-0469(1988)045<0549:VIACOM>2.0.CO;2.

- Shinoda, T., G. N. Kiladis, and P. E. Roundy (2009), Statistical representation of equatorial waves and tropical instability waves in the Pacific Ocean, *Atmos. Res.*, *94*, 37–44, doi:10.1016/j.atmosres.2008.06.002.
- Takayabu, Y. N., T. Iguchi, M. Kachi, A. Shibata, and H. Kanzawa (1999), Abrupt termination of the 1997–98 El Niño in response to a Madden-Julian oscillation, *Nature*, *402*, 279–282, doi:10.1038/46254.
- Tang, W., and W. T. Liu (1996), *Objective Interpolation of Scatterometer Winds*, *JPL Publ. 96-19*, 16 pp., Jet Propul. Lab., Pasadena, Calif.
- Tozuka, T., T. Kagimoto, Y. Masumoto, and T. Yamagata (2002), Simulated multiscale variations in the western tropical Pacific: The Mindanao Dome revisited, *J. Phys. Oceanogr.*, *32*, 1338–1359, doi:10.1175/1520-0485(2002)032<1338:SMVITW>2.0.CO;2.
- Trenberth, K. E., and D. P. Stepaniak (2001), Indices of El Niño evolution, *J. Clim.*, *14*, 1697–1701, doi:10.1175/1520-0442(2001)014<1697:LIOENO>2.0.CO;2.
- Wang, B., and Q. Zhang (2002), Pacific–East Asian teleconnection. Part II: How the Philippine sea anomalous anticyclone is established during El Niño development, *J. Clim.*, *15*, 3252–3265, doi:10.1175/1520-0442(2002)015<3252:PEATPI>2.0.CO;2.
- Wang, C. (2001), A unified oscillator model for the El Niño–Southern Oscillation, *J. Clim.*, *14*, 98–115, doi:10.1175/1520-0442(2001)014<0098:AUOMFT>2.0.CO;2.
- Wang, C., and J. Picaut (2004), Understanding ENSO physics—A review, in *Earth's Climate: The Ocean–Atmosphere Interaction*, *Geophys. Monogr. Ser.*, vol. 147, pp. 21–48, AGU, Washington, D. C.
- Wang, G., and H. H. Hendon (2007), Sensitivity of Australian rainfall to inter–El Niño variations, *J. Clim.*, *20*, 4211–4226, doi:10.1175/JCLI4228.1.
- Weisberg, R. H., and C. Wang (1997), A western Pacific oscillator paradigm for the El Niño–Southern Oscillation, *Geophys. Res. Lett.*, *24*, 779–782, doi:10.1029/97GL00689.
- Weng, H., S. K. Behera, and T. Yamagata (2009), Anomalous winter climate conditions in the Pacific Rim during recent El Niño Modoki and El Niño events, *Clim. Dyn.*, *32*, 663–674, doi:10.1007/s00382-008-0394-6.
- Yeh, S.-W., J.-S. Kug, B. Dewitte, M.-H. Kwon, B. P. Kirtman, and F.-F. Jin (2009), El Niño in a changing climate, *Nature*, *461*, 511–514, doi:10.1038/nature08316.
- Zhang, R., A. Sumi, and M. Kimoto (1996), Impact of El Niño on the East Asian monsoon: A diagnostic study of the 86–87 and 91–92 events, *J. Meteorol. Soc. Jpn.*, *74*, 49–62.
- Zhang, Z., and T. N. Krishnamurti (1996), A generalization of Gill's heat-induced tropical circulation, *J. Atmos. Sci.*, *53*, 1045–1052, doi:10.1175/1520-0469(1996)053<1045:AGOGHI>2.0.CO;2.

H. E. Hurlburt, E. J. Metzger, and T. Shinoda, Naval Research Laboratory, Code 7323, Bldg. 1009, Stennis Space Center, MS 39529, USA. (toshiaki.shinoda@nrlssc.navy.mil)